Chem Biol Drug Des 2016

Research Article

Discovery of New Substrates for *LuxAB* Bacterial Bioluminescence

Tianyu Jiang[1], Weishan Wang[2], Xingkang Wu[3], Wenxiao Wu[1], Haixiu Bai[1], Zhao Ma[1], Yuemao Shen[3], Keqian Yang[2,*] and Minyong Li[1,*]

[1]Department of Medicinal Chemistry, Key Laboratory of Chemical Biology (MOE), School of Pharmaceutical Sciences, Shandong University, Jinan, Shandong 250012, China
[2]State Key Laboratory of Microbial Resources, Institute of Microbiology, Chinese Academy of Sciences, Beijing 100190, China
[3]Department of Natural Products, Key Laboratory of Chemical Biology (MOE), School of Pharmaceutical Sciences, Shandong University, Jinan, Shandong 250012, China
**Corresponding authors: Keqian Yang, yangkq@im.ac.cn; Minyong Li, mli@sdu.edu.cn*

In this article, four novel substrates with long halftime have been designed and synthesized successfully for *luxAB* bacterial bioluminescence. After *in vitro* and *in vivo* biological evaluation, these molecules can emit obvious bioluminescence emission with known bacterial luciferase, thus indicating a new promising approach to developing the bacterial bioluminescent system.

Key words: bacterial bioluminescence, imaging, *luxAB*, new long-chain aliphatic aldehydes

Received 31 May 2015, revised 26 November 2015 and accepted for publication 8 February 2016

Bioluminescence, as a particular form of chemiluminescence, is a natural phenomenon that emits visible light resulted from the reaction catalyzed by corresponding luciferase. Bioluminescence exists in most life-forms (1), for example, firefly, bacteria, fungi, and marine vertebrates and invertebrates. Bioluminescent technology has drawn more and more attention because of its wide application in the detection and imaging of biological process *in vitro* and *in vivo* (2,3). Considering that the occurrence of bioluminescence does not demand an excitation light source as compared to fluorescence, this method has low background interference.

As the widespread prevalence in the marine environment, luminous bacteria have been isolated from multiple sources, including seawater, the light organs of marine luminous organisms and some symbiotic organisms of animals. So far, there are three major genera of luminous bacteria, including *Vibrio*, *Photobacterium*, and *Photorhabdus* (*Xenorhabdus*) (4–6). Luminescence is an especially striking activity controlled by gene regulation called quorum sensing in *Vibrio* (7,8). Quorum sensing (QS) is a cell-to-cell communication that regulates gene expression and coordinates their behavior in line with the cell population density as a result of discerning molecules named autoinducers (AIs) (9). For example, the typical LuxR–LuxI quorum sensing system plays a significant role in the gene response of light production in *Vibrio fischeri* (10). The *Vibrio* bacterial bioluminescence reaction starts with oxidation of reduced flavin and a long-chain aliphatic (C10–C12) aldehyde that can be catalyzed by the corresponding luciferase. It should be underlined that the *Vibrio* bacterial bioluminescence is always bursting to reach the peak with a very fast speed. The concomitant maximum emission peaks of the bioluminescence reaction of various bacterial species are usually ranging from the wavelength of 472–500 nm. In this case, the aldehyde is regarded as a luciferin to some extent (11,12).

It is known that the *Vibrio* bacterial luciferase is encoded by *lux* gene cassette that consists of a set of genes (13–15). The *Vibrio* bacterial luciferase protein is a heterodimer formed from the products of adjacent *luxA* and *luxB* genes (16). The fatty acid reductase multienzyme complex is encoded by the gene of *luxC*, *luxD,* and *luxE*, which catalyzes the synthesis of a long-chain aldehyde (the substrate for the luciferase reaction) from the fatty acid (4,11). The product of *luxG* is a flavin reductase that regulates the regeneration of the reduced flavin mononucleotide in bioluminescence reaction (17).

The bacterial *lux* operon is an important bioreporter system that has been expanded for the detection of chemical signal molecules and imaging within a living host using cooled charge-coupled device (CCD) camera. Moreover, either full or parts of them (*luxAB*) could express in alternative host organisms such as *Escherichia coli* (13,15,18). After several decades of research, great contribution has been made to the development of modified *lux* gene cassette expressing in various prokaryotic cell lines even the eukaryotic cell line (19).

 doi: 10.1111/cbdd.12747

However, hitherto little work has been done in exploring the new substrates of the bacterial bioluminescence. Nowadays, the conventional substrates of bacterial bioluminescence are long-chain aliphatic aldehydes from natural source such as decanal, dodecanal, and tetradecanal (11). To fill this gap, herein we undertake an effort in designing a new series of compounds (**5a**, **5b**, **9a**, **9b**, **11a**, and **11b**) with the property of fluorescence as the luciferin derivatives involved in the bacterial bioluminescence. Substituted 1,8-naphthalimide and 2,1,3-benzoxadiazole groups were chosen to be introduced in the structures of novel compounds. We want to probe and discuss the characteristics of bioluminescent and optical variation induced by introduction of fluorescent groups in order to obtain the better luciferin for bacterial bioluminescence.

Methods and Materials

Materials and instruments

All reagents and solvents available were used as received unless otherwise noted. All reactions were monitored by TLC with 0.25-mm silica gel plates (60GF-254). UV light, iodine stain, and ninhydrin were used to visualize the spots. Silica gel was utilized for column chromatography purification. ^{1}H NMR and ^{13}C-NMR were recorded on a Bruker DRX spectrometer at 300 or 400 MHz, δ in parts per million and J in hertz, using TMS as an internal standard. ESI-MS spectra were recorded on an API 4000 spectrometer (AppliedBiosystems, Foster city, CA, USA). Melting points were determined uncorrected on an electrothermal melting point apparatus. HPLC tests were performed with Agilent Technologies 1260 liquid chromatography (Singapore City, Singapore). Water used for the fluorescence and bioluminescence studies was doubly distilled and further purified with a Mill-Q filtration system (Millipore, Watertown, MA, USA). Bioluminescence measurements were determined with an IVIS Kinetic (Caliper Life Sciences, Hopkinton, MA, USA) equipped with a cooled charge-coupled device (CCD) camera for bioluminescent imaging. Bioluminescence spectra were measured with F-2500 FL Spectrophotometer (HITACHI High technologies Corporation, Tokyo, Japan). Decanal used in bioluminescence assay was purchased from Sigma (Shanghai, China).

Organic synthesis of novel substrates

We have synthesized six novel compounds as described in Scheme 1.

The preparation of 2-(10-hydroxydecyl)isoindoline-1, 3-dione (**1a**):

To a stirred solution of 10-bromodecanol (800 mg, 3.37 mmol) in dimethylformamide (DMF) was added potassium naphthalimide (687 mg, 3.71 mmol). The reaction mixture was refluxed at 80 °C for 2 h and then cooled to the room temperature. After that, water was added to the mixture, and precipitation of crude product was collected by filtration and washed with water. The product was recrystallized from a mixture of dichloromethane and petroleum ether and then was dried in vacuo to afford 1 g of pure product (**1a**) as a pale powder. Yield: 98%. Mp 62–64 °C. ^{1}H NMR (400 MHz, $CDCl_3$): δ 7.84 (m, 2H), 7.71 (m, 2H), 3.65 (m, 4H), 1.67 (m, 2H), 1.55 (m, 2H), 1.33~1.28 (m, 12H). ESI-MS: m/z 304.5 $[M + H]^+$, 321.5 $[M + NH_4]^+$, 326.5 $[M + Na]^+$.

2-(12-hydroxydodecyl)isoindoline-1,3-dione (**1b**): pale powder; yield 98%. Mp 63–65 °C. ^{1}H NMR (400 MHz, $CDCl_3$): δ 7.84 (m, 2H), 7.71 (m, 2H), 3.66 (m, 4H), 1.67 (m, 2H), 1.56 (m, 2H), 1.32~1.26 (m, 16H). ESI-MS: m/z 332.7 $[M + H]^+$, 349.6 $[M + NH_4]^+$, 354.5 $[M + Na]^+$.

The preparation of 10-amino-1-decanol (**2a**):

To a stirred solution of **1a** (330 mg, 0.99 mmol) in ethanol (10 mL) was added hydrazine hydrate (85%, 220 mg). The reaction mixture was refluxed at 80 °C for 2.5 h, resulting in the formation of a white precipitate. The suspension was cooled and concentrated. The white solid was triturated with dichloromethane with sonication and filtered. The trituration/sonication/filtration sequence was repeated. Then, the combined filtrates were concentrated to provide 130 mg of pale powder (**2a**). Yield: 69%. Mp 67–69 °C. ^{1}H NMR (400 MHz, $CDCl_3$) : δ 3.57 (t, J = 6.8 Hz, 2H), 2.62 (t, J = 7.2 Hz, 2H), 1.46~1.52 (m, 2H), 1.37 (m, 2H), 1.27~1.22 (m, 12H). MS: m/z 174.4 $[M + H]^+$.

12-amino-1-dodecanol (**2b**): pale powder; yield 55%; Mp 66–68 °C. ^{1}H NMR (300 MHz, $CDCl_3$) : δ 3.63 (t, J = 6.6 Hz, 2H), 2.68 (t, J = 6.9 Hz, 2H), 1.59~1.52 (m, 4H), 1.46~1.39 (m, 2H), 1.28 (m, 14H). MS: m/z 202.4 $[M + H]^+$.

The preparation of 4-*N*,*N*-(dimethyl)aminonaphthalene-1, 8-dicarboximide (**3**):

A total of 9.76 g of dimethylamine aqueous solution (40%) and a catalytic amount of $CuSO_4$ (270 mg) were added to a suspension of 4-bromonaphthalene-1,8-dicarboximide (3 g, 10 mmol) in DMF (30 mL). The mixture was then refluxed at 160 °C for 2 h, after which the solvent was evaporated under vacuum. The product **3** was crystallized from ethanol, dichloromethane, and petroleum ether as a yellow solid (20). Yield: 52%. Mp 205–207 °C. ^{1}H NMR (400 MHz, $CDCl_3$) δ 8.49 (dd, J = 7.2 Hz, 1.2 Hz, 1H), 8.41 (dd, J = 8.8 Hz, 1.2 Hz, 1H), 8.38 (d, J = 8.4 Hz, 1H), 7.61 (m, 1H),

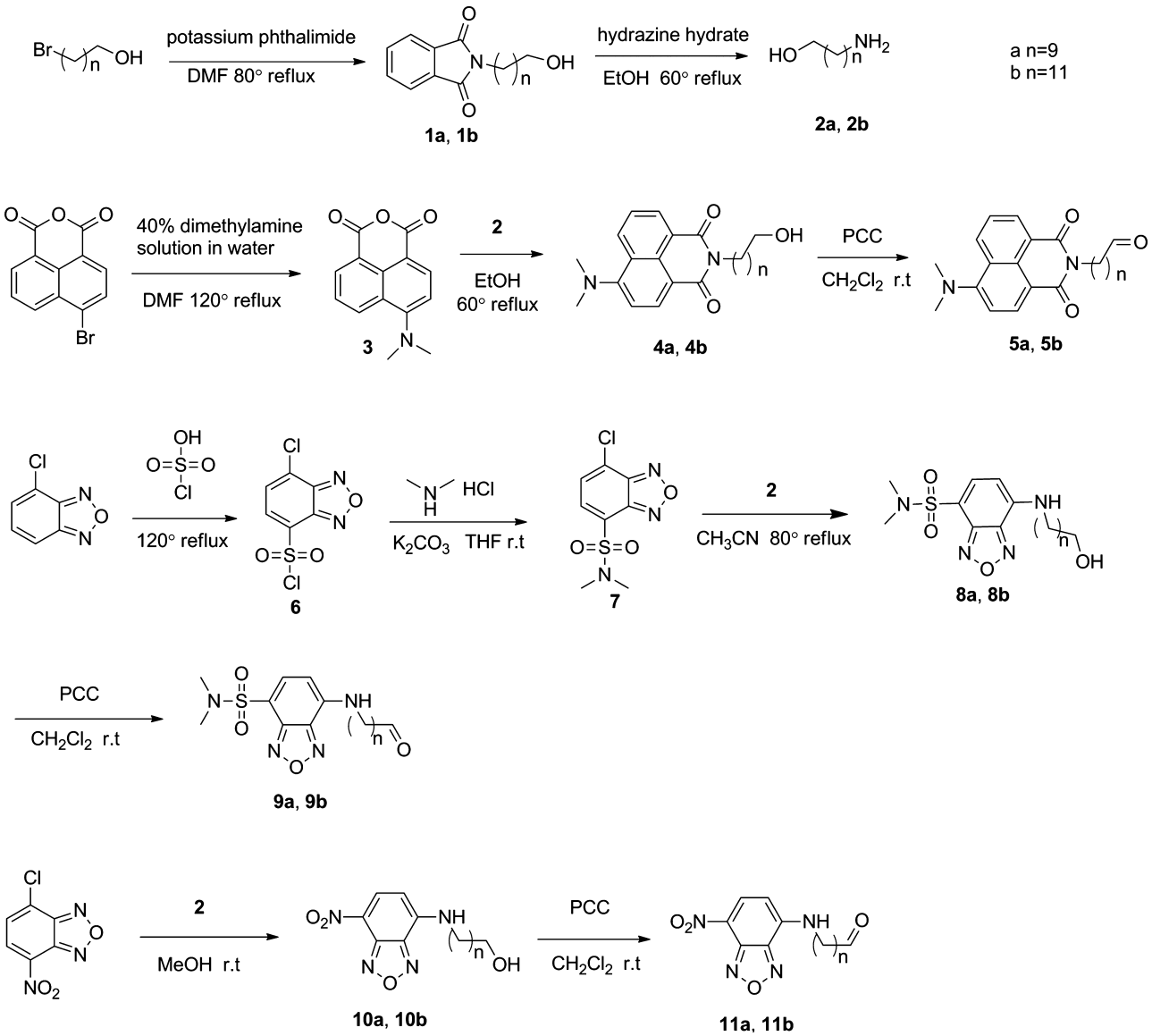

Scheme 1: Synthesis scheme of novel derivatives.

7.03 (m, 1H), 3.11 (s, 6H). MS: m/z 242.4 $[M + H]^+$, 259.3 $[M + NH_4]^+$, 264.3 $[M + Na]^+$.

The preparation of 4-*N*,*N*-(dimethyl)aminonaphthalene-9-N-(10-hydroxydecyl)-1,8-dicarboximide (**4a**):

A solution of **3** (100 mg, 414 μmol) in EtOH (3 mL) was added to a solution of **2a** (87 mg, 497 mmol) in EtOH (10 mL). The reaction was stirred and refluxed at 80 °C for 3 h. Then, the mixture was cooled to room temperature and concentrated under reduced pressure. The crude product was subjected to chromatography on silica gel (PE/EtOAC 5:1–3:1) to give yellow viscous oil. Yield: 69%. ^{1}H NMR (400 MHz, CD_3Cl) δ 8.59 (dd, J = 7.4 Hz, 1H), 8.50 (d, J = 8 Hz, 1H), 8.46 (dd, J = 8.6 Hz, 1H), 7.68 (m, 1H), 7.14 (d, J = 8.4 Hz, 1H), 4.17 (t, J = 7.6 Hz, 2H), 3.66 (m, 2H), 3.12 (s, 6H), 1.74 (m, 2H), 1.58 (m, 2H), 1.44 (m, 2H), 1.35~1.27 (m, 12H). ESI-MS m/z: 397.5 $[M + H]^+$.

4-N,N-(dimethyl)aminonaphthalene-9-N-(12-hydroxydodecyl)-1,8-dicarboximide (**4b**): yellow viscous oil. Yield: 76%. ^{1}H NMR (400 MHz $(CD_3)_2OD$) δ 8.43 (dd, J = 8.4 Hz, 1H), 8.38 (dd, J = 7.2 Hz, 1.2 Hz, 1H), 8.28 (dd, J = 8.4 Hz, 1.2 Hz, 1H), 7.63 (m, 1H), 7.13 (m, 1H), 3.98 (t, J = 7.4 Hz, 2H), 3.38 (t, J = 6.6 Hz, 2H), 3.00 (s, 6H), 1.57 (m, 2H), 1.35 (m, 2H), 1.25 (m, 2H), 1.16 (m, 12H). ESI-MS m/z: 425.6 $[M + H]^+$, 447.6 $[M + Na]^+$.

The preparation of 4-*N*,*N*-(dimethyl)aminonaphthalene-9-N-(9-aldehyde-decyl)-1,8-dicarboximide (**5a**):

To a suspension of compound **4a** (80 mg, 201 μmol) and silica gel(160 mg) in dry dichloromethane was added pyridinium chlorochromate complex (60 mg, 282 μmol) with stirring at 0 °C. Then the reaction mixture was stirred at room temperature under Ar atmosphere and protected from light overnight. The mixture was concentrated under reduced pressure and then was subjected to chromatography on silica gel (PE/EtOAC 10:1) to give very viscous yellow viscous oil. Yield: 44%. Analytical RP HPLC (Phenomenex, C8, 250 × 4.6 mm column): methanol:water 75:25, 1.5 mL/min at 440 nm, Rt: 11.177 min, 100%. ^{1}H NMR (400 MHz, $CDCl_3$) δ 9.68 (s, 1H), 8.49 (dd, J = 7.4 Hz, 1 Hz, 1H), 8.41 (d, J = 8.4 Hz, 1H), 8.36 (dd, J = 8.4 Hz, 0.8 Hz, 1H), 7.59 (m, 1H), 7.04 (d, J = 8.4 Hz, 1H), 4.08 (t, J = 7.6 Hz, 2H), 3.03 (s, 6H), 2.33 (td, J = 7.4 Hz, 1.9 Hz, 2H), 1.65 (m, 2H), 1.54~1.47 (m, 2H), 1.36~1.32 (m, 2H), 1.29~1.23 (m, 8H). ^{13}CNMR (100 MHz, $CDCl_3$) δ 201.9, 163.6, 163.1, 155.9, 131.6, 130.1, 129.9, 129.2, 124.3, 123.9, 122.2, 114.2, 112.3, 43.8, 43.9, 39.2, 28.3, 28.3, 28.1, 27.1, 26.1. HR-MS: m/z calcd for $[C_{24}H_{30}N_2O_3 + H]^+$ 395.2335, found: 395.2323 $[M + H]^+$.

4-*N*,*N*-(dimethyl)aminonaphthalene-9-N-(11-aldehyde-dodecyl)-1,8-dicarboximide (**5b**): very viscous yellow viscous oil; yield: 46%. Analytical RP HPLC (Phenomenex, C8, 250 × 4.6 mm column): methanol:water 80:20, 1.5 mL/min at 440 nm, Rt: 10.654 min, 100%. ^{1}H NMR (400 MHz, $CDCl_3$) : δ 9.76 (s, 1H), 8.57 (d, J = 7.2 Hz, 1H), 8.48 (d, J = 8.4 Hz, 1H), 8.44 (d, J = 8.4 Hz, 1H), 7.67 (t, J = 7.8 Hz, 1H), 7.13 (d, J = 8.4 Hz, 1H), 4.15 (t, J = 7.6 Hz, 2H), 3.11 (s, 6H), 2.42 (td, J = 7.3 Hz, 1.7 Hz, 2H), 1.73~1.68 (m, 2H), 1.64~1.60 (m, 2H), 1.43~1.26 (m, 14H). ^{13}CNMR (100 MHz, $CDCl_3$) δ 203.0, 164.6, 164.1, 156.9, 132.6, 131.1, 131.0, 130.2, 125.4, 124.9, 123.2, 115.2, 113.4, 44.8, 43.9, 40.3, 29.7, 29.5, 29.4, 29.3, 29.2, 28.2, 27.2, 22.1. HR-MS: m/z calcd for $[C_{26}H_{34}N_2O_3 + H]^+$: 423.2648, found: 423.2640 $[M + H]^+$.

The preparation of 4-chloro-7-chlorosulfonic-2,1,3-benzoxadiazole (**6**):

A total of 4 mL of chlorosulfonic acid was added dropwise to 4-chloro-2,1,3-benzoxadiazole (0.6 g, 3.88 mmol) in a round bottom flask at 0. After completion, the reaction mixture was heated at 120 °C for 8 h under Ar atmosphere. The reaction mixture was dropwise poured into ice water, and the precipitation of crude product was collected by filtration and washed with water. The product **6** (0.59 g) was crystallized from dichloromethane and petroleum ether as a light brown crystal. Compound 6 was used in the next step without further purification (21). Yield: 60%. ^{1}H NMR (400 MHz, $CDCl_3$): δ 8.21 (d, J = 8 Hz, 1H), 7.68 (d, J = 8 Hz, 1H). ESI-MS: m/z 233.1 $[M–Cl + OH]^-$.

The preparation of 4-chloro-7-*N*,*N*-dimethylsulfonic-2,1,3-benzoxadiazole (**7**):

To a bottom flask containing 10 mL dried anhydrous THF, dimethylamine hydrochloride (116 mg, 1.42 mmol) and K_2CO_3 (197 mg, 1.42 mmol) were dissolved and stirred at room temperature for 30 min. Then, the solution above was added dropwise to the THF solution of compound **6** with stirring at 0 °C. After the addition, the solution was further stirred for 6 h at room temperature. After removal of solvent in vacuo, the residue was purified by silica gel column chromatography (PE/EtOAC 5:1) to afford compound **7** (190 mg) as a white powder (22). Yield: 61%. ^{1}H NMR (400 MHz, $CDCl_3$): δ 7.97 (d, J = 7.6 Hz, 1H), 7.56 (d, J = 7.2 Hz, 1H), 2.97 (s, 6H). ESI-MS: m/z 262.3 $[M + H]^+$, 279.3 $[M + NH_4]^+$, 284.3 $[M + Na]^+$.

The preparation of 4-N-(10-hydroxydecyl)-7-*N*,*N*-dimethylsulfonic-2,1,3-benzoxadiazole (**8a**):

To a solution of compound **2a** (60 mg, 347 μmol) in acetonitrile with stirring, was added dropwise the solution of compound **7** (70 mg, 267 μmol). Then, the mixture was refluxed at 60 °C for 8 h. After removing the solvent *in vacuo*, the residue was purified by silica gel column chromatography (PE/EtOAC 5:2) to afford compound 8a as a yellow powder (59 mg, 55%). Mp 83–85 °C. ^{1}H NMR (400 MHz, $CDCl_3$) : δ 7.83 (d, J = 8 Hz, 1H), 6.05 (d, J = 8 Hz, 1H), 5.57 (t, J = 5 Hz, 1H), 3.57 (m, 2H), 3.32 (m, 2H), 2.80 (s, 6H), 1.74~1.66 (m, 2H), 1.52~1.46 (m, 2H), 1.41~1.35 (m, 2H), 1.29~1.25 (m, 10H). ESI-MS: m/z 399.4 $[M + H]^+$, 416.5 $[M + NH_4]^+$, 421.4 $[M + Na]^+$.

4-N-(12-hydroxydodecyl)-7-*N*,*N*-dimethylsulfonic-2,1,3-benzoxadiazole (**8b**): yellow powder; yield: 50%. Mp 73–75 °C. ^{1}H NMR (400 MHz, $CDCl_3$) : δ 7.83 (d, J = 8 Hz, 1H), 6.05 (d, J = 8 Hz, 1H), 5.57 (t, J = 5.4 Hz, 1H), 3.56 (s, 2H), 3.31 (m, 2H), 2.80 (s, 6H), 1.72~1.66 (m, 2H), 1.51~1.46 (m, 2H), 1.40~1.35 (m, 2H), 1.27~1.22 (m, 14H). ESI-MS: m/z 427.5 $[M + H]^+$, 444.7 $[M + NH_4]^+$, 449.5 $[M + Na]^+$.

The preparation of 4-N-(9-aldehyde-decyl)-7-*N*,*N*-dimethylsulfonic-2,1,3-benzoxadiazole (**9a**):

To a suspension of compound **8a** (45 mg, 113 μmol) and silica gel (100 mg) in dry dichloromethane was added pyridinium chlorochromate complex (36 mg,

167 μmol) with stirring at 0 °C. Then, the reaction mixture was stirred at room temperature under Ar atmosphere and protected from light overnight. The mixture was concentrated under reduced pressure and then was subjected to chromatography on silica gel (PE/EtOAC 5:1) to give yellow powder (25 mg, 32%). Analytical RP HPLC (Phenomenex, C8, 250 × 4.6 mm column): methanol:water 65:35, 1.5 mL/min at 440 nm, Rt: 10.098 min, 99%. Mp 80–82 °C. ^{1}H NMR (400 MHz, $CDCl_3$) δ 9.79 (s, 1H), 7.92(d, *J* = 8 Hz, 1H), 6.14 (d, *J* = 8 Hz, 1H), 5.64 (t, *J* = 5 Hz, 1H), 3.40 (m, 2H), 2.89 (s, 6H), 2.46 (td, *J* = 7.2 Hz, 1.8 Hz, 2H), 1.81~1.75 (m, 2H), 1.67~1.64 (m, 2H), 1.48~1.44 (m, 2H), 1.41~1.35 (m, 8H). ^{13}CNMR (75 MHz, $CDCl_3$) δ 202.8, 146.3, 144.4, 140.7, 139.6, 109.4, 98.7, 43.9, 43.6, 37.8, 29.2, 29.2, 29.1, 28.6, 27.0, 22.0. HR-MS: m/z calcd for $[C_{18}H_{28}N_4O_4S + H]^+$: 397.1910, found: 397.1901 $[M + H]^+$.

4-N-(11-aldehyde-dodecyl)-7-*N*,*N*-dimethylsulfonic-2,1,3-benzoxadiazole (**9b**): yellow powder; yield: 43%. Analytical RP HPLC (Phenomenex, C8, 250 × 4.6 mm column): methanol:water 70:30, 1.5 mL/min at 440 nm, Rt: 11.663 min, 99%. Mp 78–79 °C. ^{1}H NMR (400 MHz, $CDCl_3$) δ 9.79 (t, *J* = 1.8 Hz, 1H), 7.92 (d, *J* = 8 Hz, 1H), 6.14 (d, *J* = 8 Hz, 1H), 5.65 (t, *J* = 4.8 Hz, 1H), 3.40 (m, 2H), 2.89 (s, 6H), 2.45 (td, *J* = 7.3 Hz, 1.7 Hz, 2H), 1.82~1.76 (m, 2H), 1.69~1.62 (m, 2H), 1.49~1.44 (m, 2H), 1.38~1.32 (m, 12H). ^{13}CNMR (100 MHz, $CDCl_3$) δ 202.8, 146.3, 144.5, 140.7, 139.6, 109.5, 98.7, 43.9, 43.6, 37.8, 29.4, 29.3, 29.3, 29.2, 29.1, 28.6, 27.0, 22.1. HR-MS: m/z calcd for $[C_{20}H_{32}N_4O_4S + H]^+$: 425.2223, found: 425.2212 $[M + H]^+$.

The preparation of 4-N-(10-hydroxydecyl)-7-nitro-2,1,3-benzoxadiazole (**10a**):

To a stirred solution of compound **2a** (24 mg, 140 μmol) in methanol was added dropwise the solution of 4-chloro-7-nitro-1,2,3-benzoxadiazole (28 mg, 140 μmol). Then, the mixture was further stirred at room temperature overnight. After removing the solvent *in vacuo*, the residue was purified by silica gel column chromatography (PE/EtOAC 10:3) to afford compound **10a** as an orange powder (30 mg, 64%). Mp 104–105 °C. ^{1}H NMR (400 MHz, $CDCl_3$) δ 8.51 (d, *J* = 8.4 Hz, 1H), 6.17 (d, *J* = 8.4 Hz, 1H), 3.65 (t, *J* = 6.6 Hz, 2H), 3.48 (m, 2H), 1.81 (m, 2H), 1.59 (m, 2H), 1.47 (m, 2H), 1.37 (m, 8H), 1.25 (m, 2H). ESI-MS: m/z 337.6 $[M + H]^+$, 354.5 $[M + NH_4]^+$, 359.6 $[M + Na]^+$.

4-N-(12-hydroxydecyl)-7-nitro-2,1,3-benzoxadiazole (**10b**): orange powder; yield: 45%; Mp 108–109 °C. ^{1}H NMR (400 MHz, $CDCl_3$) δ 8.50 (d, *J* = 8.4 Hz, 1H), 6.24 (s, 1H), 6.17 (d, *J* = 8.4 Hz, 1H), 3.65 (t, *J* = 6.6 Hz, 2H), 3.49 (m, 2H), 1.81 (m, 2H), 1.47 (m, 2H), 1.29 (m, 16H). ESI-MS: m/z 365.5 $[M + H]^+$, 382.6 $[M + NH_4]^+$, 387.5 $[M + Na]^+$.

The preparation of 4-N-(9-aldehyde-decyl)-7-nitro-2,1,3-benzoxadiazole (**11a**):

To a suspension of compound **10a** (50 mg, 149 μmol) and silica gel (100 mg) in dry dichloromethane was added pyridinium chlorochromate complex (45 mg, 208 μmol) with stirring at 0 °C. Then, the reaction mixture was stirred at room temperature under Ar atmosphere and protected from light overnight. The mixture was concentrated under reduced pressure and then was subjected to chromatography on silica gel (PE/EtOAC 10:1) to give orange powder (20 mg, 41%). Analytical RP HPLC (Phenomenex, C8, 250 × 4.6 mm column): methanol:water 60:40, 1.0 mL/min at 440 nm, Rt: 24.400 min, 99%. Mp: 91–92 °C. ^{1}H NMR (300 MHz, $CDCl_3$) δ 9.77(s, 1H), 8.48 (d, *J* = 8.7 Hz, 1H), 6.31 (s, 1H), 6.18 (d, *J* = 8.7 Hz, 1H), 3.50 (m, 2H), 2.44 (td, *J* = 7.2 Hz, 1.2 Hz, 2H), 1.82 (m, 2H), 1.64 (m, 2H), 1.46 (m, 2H), 1.33 (m, 8H). ^{13}CNMR (100 MHz, $CDCl_3$) δ 202.8, 144.3, 143.9, 143.9, 136.5, 124.0, 98.5, 44.0, 43.9, 29.2, 29.1, 29.0, 28.5, 26.9, 22.0. HR-MS: m/z calcd for $[C_{16}H_{22}N_4O_4 + H]^+$: 335.1719, found: 335.1717 $[M + H]^+$.

4-N-(11-aldehyde-decyl)-7-nitro-2,1,3-benzoxadiazole (**11b**): orange powder; yield: 51%; Analytical RP HPLC (Phenomenex, C8, 250 × 4.6 mm column): methanol: water 60:40, 1.0 mL/min at 440 nm, Rt: 21.591 min, 99%. Mp: 98–99 °C. ^{1}H NMR (300 MHz, $CDCl_3$) δ 9.77 (t, *J* = 1.6 Hz, 1H), 8.49 (d, *J* = 8.7 Hz, 1H), 6.32 (s, 1H), 6.18 (d, *J* = 8.4 Hz, 1H), 3.50 (m, 2H), 2.43 (td, *J* = 7.2 Hz, 1.7 Hz, 2H), 1.82 (m, 2H), 1.61 (m, 2H), 1.48~1.40 (m, 2H), 1.30 (m, 12H). ^{13}CNMR (100 MHz, $CDCl_3$) δ 202.9, 144.3, 143.9, 143.9, 136.4, 124.1, 98.5, 44.0, 43.9, 29.7, 29.4, 29.3, 29.2, 29.1, 28.6, 26.9, 22.0. HR-MS: m/z calcd for $[C_{18}H_{26}N_4O_4 + H]^+$: 363.2032, found: 363.2026 $[M + H]^+$.

Compounds **5a, 5b, 9a, 9b, 11a,** and **11b** should be kept with N_2 at −20 °C for a long-time store.

Fluorescence spectra measurement

A 95% ethanol stock solution of the respective new substrate (10 mM) was diluted to the corresponding concentration with PBS (50 mM, pH 7.0). The PBS solution of the compound (200 μM, 150 μL) was added to a 96-well black flat-bottom microscale plate and then scanned with the Thermo Scientific Varioskan Flash microplate reader (Thermo Electron Corporation, Waltham, MA, USA).

Construction of the plasmid pCS26-luxAB

The 5935-bp fragment was obtained by PCR using primers luxABF and luxABR from pK316 (23), and then, the fragment was self-ligated using the Gibson assembly method (24) to generate the plasmid pCS26-luxAB, in which luxAB is under the control of kasOp* promoter (Figure S2).

The primers used in the construction were as follows:

luxABF: agagtgaggaaccctcgaggggatcctctagttgcg.

luxABF: agagtgaggaaccctcgaggggatcctctagttgcg.

Bioluminescence assay

To determine the bioluminescence properties of the novel derivatives, plasmids pCS26-luxAB encoding bacterial luciferase (*luxAB*) were transfected into *E. coli* cultured in the plate. Specifically, *E. coli* was streak-seeded on fresh LB plates and then cultured in the presence of 25 μg/mL kanamycin. Colonies appeared after overnight incubation at 37 °C. A single colony was picked from the LB plate. Then, this strain was grown overnight with aeration (250 rpm) at 37°C in 5 mL of LB medium with antibiotics (20 μg/mL kanamycin) to OD_{600} 1.2–1.4. The *E. coli* cultures were washed twice with fresh M9 medium, and then, the cell pellet was resuspended in fresh M9 medium and diluted to OD_{600} 1.0. The *E. coli* culture was prepared for each measurement.

All compounds were freshly dissolved in and diluted to appropriate concentrations in PBS (50 mM, pH 7.0) with a little addition of 95% EtOH (final ethanol concentration <0.5% v/v) for each measurement. In all the measurements, the final ethanol concentration in the sample solution was kept constant at 0.5% (v/v) to avoid the effect of ethanol on the BL reaction. To measure bioluminescence intensity, the solution of compound (40 μL) was added to a 96-well black flat-bottom microscale plate and then the fresh *E. coli* cultures (80 μL) was added and mixed quickly. Bioluminescence intensities of native decanal and the derivatives were immediately measured with an IVIS Kinetic (Caliper Life Sciences) equipped with a cooled charge-coupled device (CCD) camera with the exposure time of 60 seconds. The measurement would last 20–30 min to determine the kinetic profiles of bioluminescence at different concentrations.

For the recording of bioluminescence spectra and relative quantum yields (RQYs), an aliquot of the *E. coli* culture (300 μL) with OD_{600} 1.0 was mixed with PBS (150 μL) containing decanal (0.5 mM) or derivative (1 mM) in a quartz cell and the mixture was immediately measured with a F-1200 fluorescence spectrophotometer in luminescence mode with the lamp off at a scan rate of 3000 nm/min. The wavelengths of maximal bioluminescence intensities (λ_{max}) and the quantitative bioluminescence spectra were determined using the instrument software (FL SOLUTIONS ver. 2.1). The quantum yield (QY) was calculated by dividing the measured total number of photons by the number of substrate molecules in the solution (25,26).

In vivo *Imaging*

Novel substrates **5a** and **5b** were chosen for bioluminescence imaging in mice. All compounds were freshly dissolved in and diluted to appropriate concentrations in 0.9% NaCl with a little addition of 95% EtOH (final ethanol concentration <0.5% v/v) for this measurement. The fresh *E. coli* culture was prepared as the same way of bioluminescence measurement. To demonstrate this functionality, 8-week-old female nude mice (weight: 18 ± 2 g) were treated with anesthetic agent isoflurane and then were subcutaneously injected with solution of compound (50 μL) and then were subcutaneously injected with *E. coli* culture (100 μL) *in situ* quickly. The bioluminescence was detected at once with an exposure time of 60 seconds. The next injection area of back skin would be changed after a finish of a set of subcutaneously injection.

Results and Discussion

Bioluminescence properties

Four compounds (**5a**, **5b**, **9a,** and **9b**) have the capacity to emit a significant bioluminescence light in the presence of bacterial luciferase of *Photorhabdus luminescens*. However, compounds **11a** and **11b** exhibited no response to the bacterial luciferase. Therefore, we only discussed the bioluminescent characteristics of **5a**, **5b**, **9a,** and **9b** in this article. In addition, all compounds have fluorescence properties with the maximum excitation around 460 nm and the maximum emission in the range of 547–575 nm (Figure S1).

The recognition-dependent bioluminescence properties of four new compounds were well investigated using *E. coli* that transfected with the plasmid carrying the gene *luxAB* of *Photorhabdus luminescens*, considering that the luciferase protein derived from the *lux* gene of *Photorhabdus luminescens* is more thermostable than of *Vibrio harveyi* and *Vibrio fischeri* (19).

Four of our novel compounds displayed significant bioluminescence properties with bacterial luciferase. A comparison of the bioluminescent intensities of the new molecules and decanal is depicted in Figure 1. The bioluminescence intensities of them all were weaker than that of the native decanal. However, compounds **5a** and **5b** show better intensities among them. What's more, compound **5b** displays similar intensity compared with decanal when they both were in relatively low concentrations (Figure 1B). Therefore, **5b** has an advantage over them in the emission of bacterial bioluminescence. The **5a** and **5b** were more

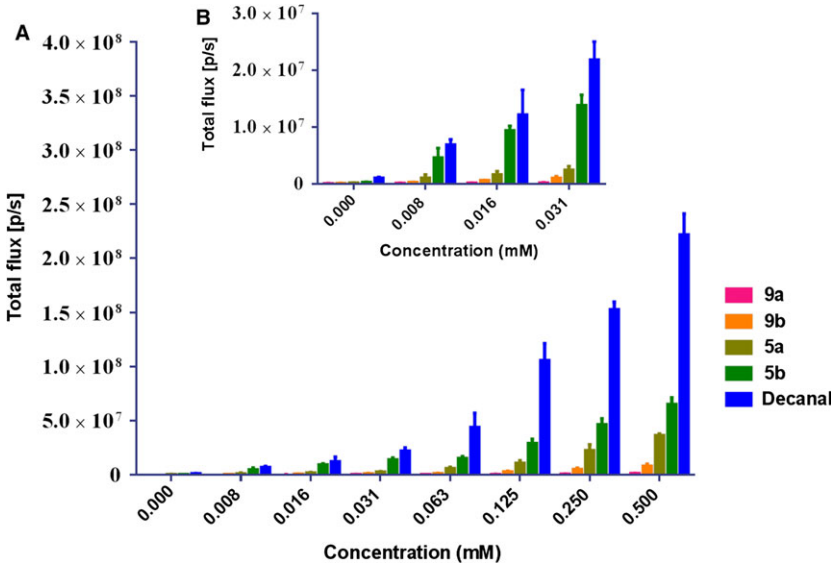

Figure 1: The comparison of bioluminescence intensities of decanal and new four derivatives (A). The (B) is the enlargement of part of (A). The values are shown by means ± SD of three independent assays.

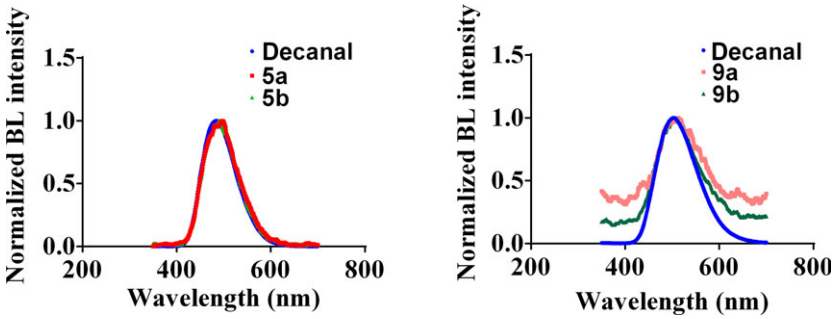

Figure 2: Bioluminescent spectra of four new derivatives and decanal.

excellent than the **9a** and **9b**, and this may be due to their better aqueous solubility and high polarity.

The comparison of the bioluminescent spectra of four new compounds and native decanal is depicted in Figure 2. The emission wavelengths of four new derivatives and native decanal are very similar. They just show tiny red-shifted emission compared to that of decanal.

To further understand the redshift level of bioluminescence induced by these molecules, we have calculated their GFP/OPEN ratio. The ratio is equal to the BL intensity that was measured with a GFP filter divided by the BL intensity at all wavelengths. It is known that the maximum emission wavelength of the GFP is at 509 nm, and luminous flux around 509 nm would be detected if a GFP filter is put on. This ratio would reflex the redshift of the substrate–luciferase bioluminescent reaction to some extent. We tested the GFP/OPEN ratio of our compounds and decanal at different concentrations using a higher sensitivity instrument (IVIS Kinetic equipped with a CCD). As shown in Figure 3, the GFP/OPEN ratios of decanal from the low to the high concentrations were all below 0.2. Meanwhile, the ratios of

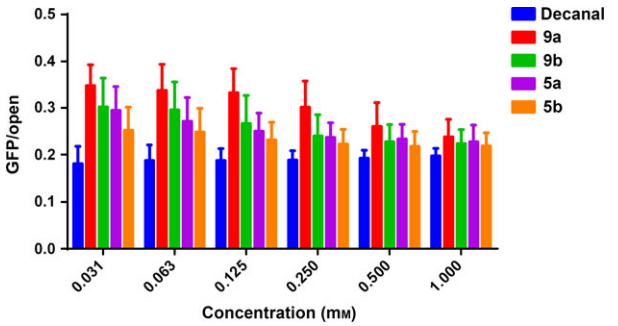

Figure 3: The GFP/OPEN ratio of all compounds at different concentrations. The values are shown by means ± SD of three independent assays performed in triplicate.

all of the molecules we synthesized were higher than 0.2, and some came to 0.3 at different concentrations. It is realized that our compounds could induce the redshift of the wavelength which involved in the bacterial bioluminescence to some extent. However, more work needs to be done to accomplish the prominent redshifted bioluminescent emission.

$$\frac{\text{GFP}}{\text{OPEN}}\text{ratio} = \frac{\text{Total flux through a GFP filter}}{\text{Total flux at all wavelengths}}$$

Moreover, we also have focused on the kinetic characteristics of our novel substrates. We evaluated the intensity–time-dependent bioluminescence (Figure 4). The bioluminescence decay halftime was calculated as shown in Table 1. We found that our compounds showed at least twofold longer halftimes than decanal. The best one (**5b**) displayed approximately threefold longer decay halftime than decanal. As we know, the bacterial bioluminescence is always bursting to reach the peak with a very fast speed and then is quenched soon. It is obvious that the bioluminescence induced by all of our compounds could decrease much slowly, which means that the persistence of our compounds is superior.

Furthermore, all of these molecules were investigated for their kinetic characteristics. By the Lineweaver–Burk plot, we have obtained the Michaelis–Menten parameters K_m and V_{max} to evaluate their combination mode with luciferase (Table 1 and Figure 5). Compound **9a** was the worst with a high K_m and a low V_{max} value. Compounds **9b** and **5a** showed moderate K_m values. The K_m of compound **5b** was near that of decanal. Further, the V_{max} values of **5b** and **5a** were similar and were basically in the same magnitude of decanal. In a word, compound **5b** showed the best kinetic characteristics. It is proved that our compounds could combine with the luciferase slowly so as to induce the bioluminescence reaction lasting longer with the low concentration.

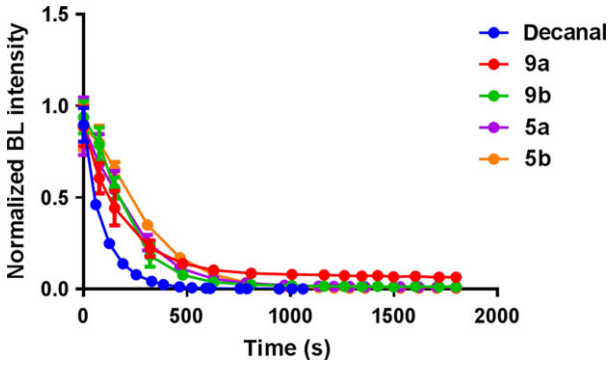

Figure 4: The kinetic profile of bioluminescence at a concentration of 0.25 mM. The values are shown by means ± SD of three independent assays.

As we all know, the quantum yield is one of the important properties of bioluminescence substrates. The relative quantum yields of all novel substrates were calculated and are exhibited in Table 1. As we can see, compound **5b** behaved best and compound **5a** took the second place among the new substrates. However, the RQY values of them were much lower than that of decanal in fact.

In vivo *imaging*

The LuxAB system has been previously used in whole animal bioluminescent imaging (16,18,19). The new substrates **5a** and **5b** could also be applied to bioluminescent imaging *in vivo* (Figure 6). The results of bioluminescence imaging in whole animal indicated that **5a** and **5b** displayed similar activities when they were confronted with decanal at the moderate concentrations in *in vivo* imaging. It is the first step to explore the new substrates that could be used in *in vivo* imaging. Because of the longer halftime of our compounds, they might have the potential to image *in vivo* for a long-lasting test.

The chemical structures of novel substrates were modified with fluorescent groups, which could make them possess optical properties. The modification with these polar groups also resulted in the change of physical state. The novel substrates were solids so as to be easier to carry and keep. In comparison with decanal, their polarity and water solubility had an improvement result from the structural modification, which might promote the interaction with luciferase. When it comes to structure–activity relationship in detail, compounds **5a** and **5b** exhibited better bioluminescence intensities and kinetic characteristics than

Table 1: The bioluminescence properties of decanal and other four new derivatives

Compounds	Decanal	**9a**	**9b**	**5a**	**5b**
BL half time (seconds)[a]	66.62	132.7	149.2	169.0	221.8
K_m[b] (mM)	0.11 ± 0.02	1.79 ± 0.42	0.72 ± 0.09	0.72 ± 0.10	0.26 ± 0.03
V_{max}[b] (s/p)	(8.42 ± 0.33) × 10^8	(7.65 ± 1.07) × 10^6	(2.35 ± 0.11) × 10^7	(9.88 ± 0.51) × 10^7	(1.07 ± 0.03) × 10^8
RQYs[c]	1	0.014	0.026	0.036	0.043

[a]BL halftime was calculated using GRAPHPAD PRISM software and taken advantage of the values when compounds were 0.25 mM.
[b]Michaelis constant K_m and maximum rate V_{max} were estimated with the Michaelis–Menten kinetics equation using GRAPHPAD PRISM software. The values are shown by means ± SD of three independent assays performed in triplicate.
[c]Relative quantum yields were obtained with a F-1200 fluorescence spectrophotometer in luminescence mode with the lamp off. The quantitative bioluminescence spectra were calculated by the instrument software FL SOLUTIONS ver. 2.1. The concentration of decanal was 0.5 mM and others were 1 mM.

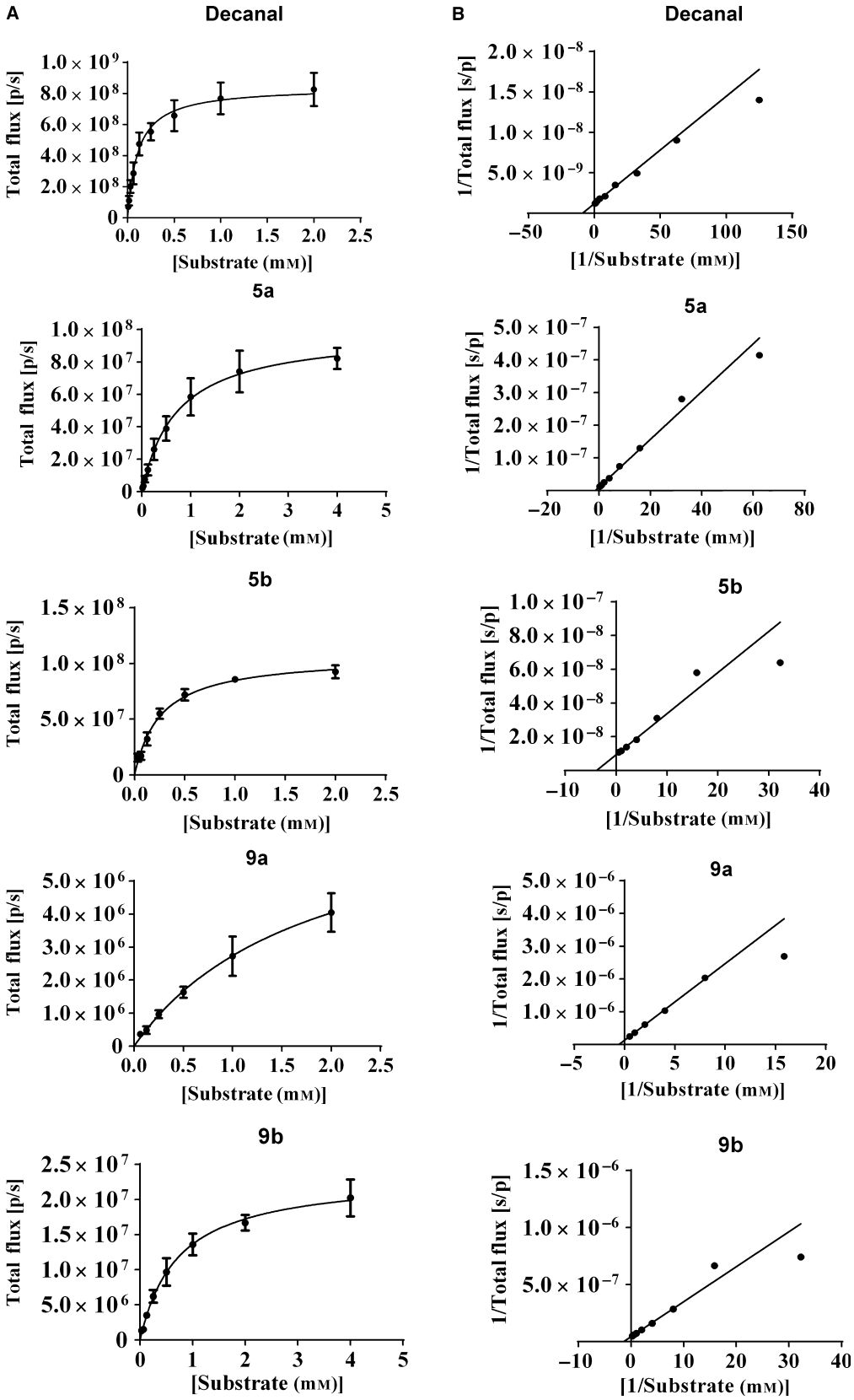

Figure 5: Kinetic characteristics of substrates. (A) Michaelis–Menten data of five compounds, and (B) the Lineweaver–Burk plot of data in (A). Both Michaelis–Menten parameters and Lineweaver–Burk plots are estimated using GRAPHPAD PRISM software.

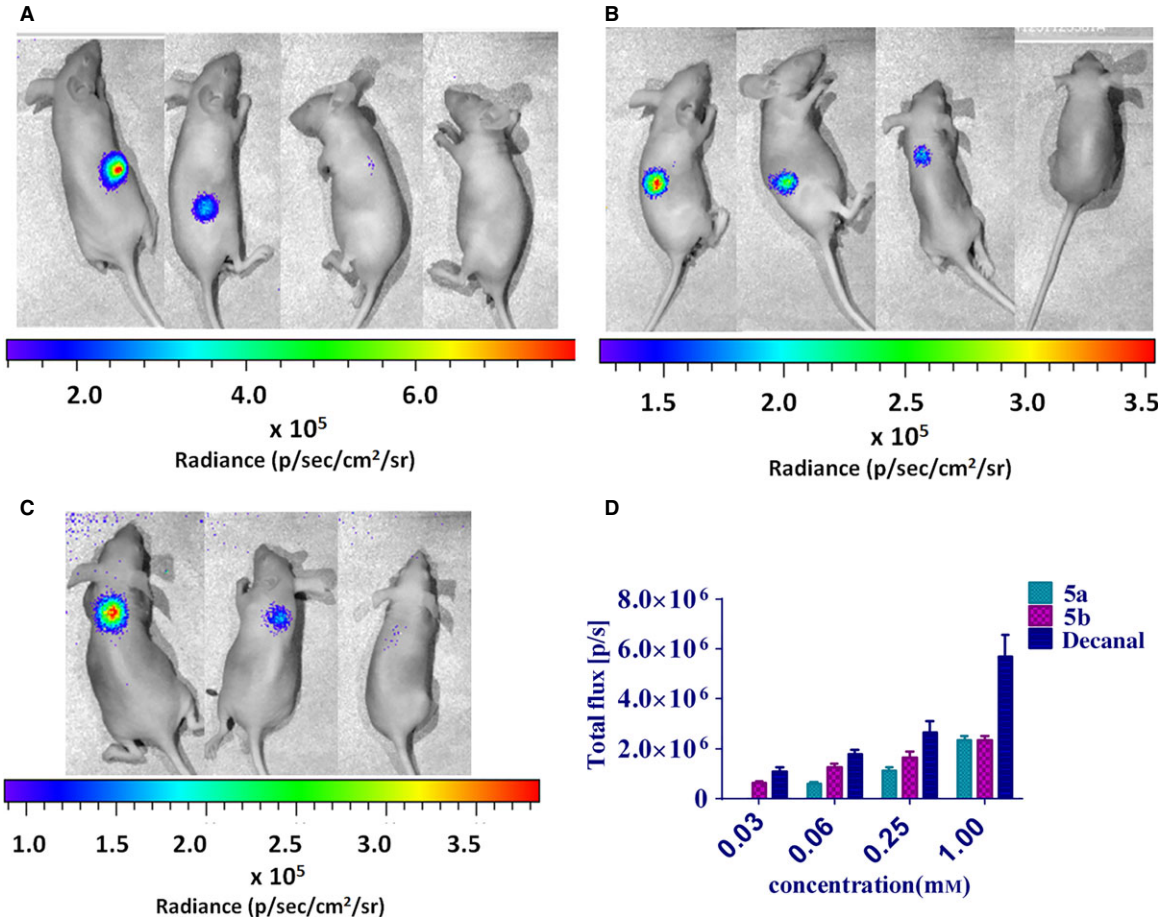

Figure 6: (A) *In vivo* imaging of decanal at 1, 0.25, 0.06, and 0.03 mM in nude mice. (B) *In vivo* imaging of **5b** at 1, 0.25, 0.06, and 0.03 mM in nude mice. (C) *In vivo* imaging of **5a** at 1, 0.25, and 0.06 mM in nude mice. (D) Quantification of total flux. The representative graphs are chosen from one experiment performed in triplicate. The error bars are SD for triplicate measurements.

9a and **9b**, which indicated that the introduction of 1,8-naphthalimide group was more appropriate compared with 2,1,3-benzoxadiazole group. In addition, **5b** seemed always to exceed **5a**, and **9b** was always better than **9a**. It is suggest that 12C aliphatic chain length was more suitable to combine with the luciferase in the bioluminescence reaction. Compounds **5a** and **5b** had the potential to be used in the animal bioluminescent imaging because their performance approached that of decanal in certain circumstances. In general, all four compounds could act as the substrates of bacterial bioluminescence although they did not surpass the conventional substrate in all aspects.

Conclusion

In this work, four types of novel bacterial bioluminescence derivatives with fluorescent property have been successfully developed. All of them showed apparent bioluminescence emission in combination with *E. coli* that transfected with a plasmid carrying *luxAB*. The bioluminescence induced by our compounds is less bright than that by decanal. The brightest emission of our compounds was observed in the case of the compound **5b**. Interestingly, they all showed much longer halftime in comparison with decanal, which suggests that our substrates could emit bioluminescence steadily and continuously.

It has been demonstrated for the first time that a structural modification of the long-chain aliphatic aldehyde can result in bacterial bioluminescence substrates with obvious bioluminescence emission. We believe that the knowledge gained through this study is of significance for the continued elucidation of the bacterial bioluminescence reaction and contributes to the development of novel bacterial bioluminescence substrates with superior optical properties.

Acknowledgments

This work was supported by grants from the National Program on Key Basic Research Project (no. 2013CB734000), the National Natural Science Foundation of China (no. 81370085), and the Independent Innovation

Foundation of Shandong University, IIFSDU (no. 2014JC008).

References

1. Li J., Chen L., Du L., Li M. (2013) Cage the firefly luciferin! – A strategy for developing bioluminescent probes. Chem Soc Rev;42:662–676.
2. Wu W., Li J., Chen L., Ma Z., Zhang W., Liu Z., Cheng Y., Du L., Li M. (2014) Bioluminescent probe for hydrogen peroxide imaging in vitro and in vivo. Anal Chem;86:9800–9806.
3. Li J., Chen L., Wu W., Zhang W., Ma Z., Cheng Y., Du L., Li M. (2014) Discovery of bioluminogenic probes for aminopeptidase N imaging. Anal Chem;86:2747–2751.
4. Close D., Xu T., Smartt A., Rogers A., Crossley R., Price S., Ripp S., Sayler G. (2012) The evolution of the bacterial luciferase gene cassette (lux) as a real-time bioreporter. Sensors (Basel);12:732–752.
5. Hastings J.W., Nealson K.H. (1977) Bacterial bioluminescence. Annu Rev Microbiol;31:549–595.
6. Makemson J., Hastings J.W. (1979) Inhibition of bacterial bioluminescence by pargyline. Arch Biochem Biophys;196:396–402.
7. Dunlap P.V. (1999) Quorum regulation of luminescence in Vibrio fischeri. J Mol Microbiol Biotechnol;1:5–12.
8. Miller M.B., Bassler B.L. (2001) Quorum sensing in bacteria. Annu Rev Microbiol;55:165–199.
9. Jiang T., Li M. (2013) Quorum sensing inhibitors: a patent review. Expert Opin Ther Pat;23:867–894.
10. Miyashiro T., Ruby E.G. (2012) Shedding light on bioluminescence regulation in Vibrio fischeri. Mol Microbiol;84:795–806.
11. Tinikul R., Chaiyen P. (2014) Structure, mechanism, and mutation of bacterial luciferase. In: Thouand G., Marks R., editors. Bioluminescence: Fundamentals and Applications in Biotechnology - Volume 3, Volume 154 of the series. Adv Biochem Eng Biotechnol. Berlin: Springer; p. 47–74.
12. Tu S.-C., Mager H.I.X. (1995) Biochemistry of bacterial bioluminescence. Photochem Photobiol;62:615–624.
13. Belas R., Mileham A., Cohn D., Hilman M., Simon M., Silverman M. (1982) Bacterial bioluminescence: isolation and expression of the luciferase genes from Vibrio harveyi. Science;218:791–793.
14. Engebrecht J., Nealson K., Silverman M. (1983) Bacterial bioluminescence: isolation and genetic analysis of functions from Vibrio fischeri. Cell;32:773–781.
15. Cohn D.H., Mileham A.J., Simon M.I., Nealson K.H., Rausch S.K., Bonam D., Baldwin T.O. (1985) Nucleotide sequence of the luxA gene of Vibrio harveyi and the complete amino acid sequence of the alpha subunit of bacterial luciferase. J Biol Chem;260:6139–6146.
16. Gahan C.G. (2012) The bacterial lux reporter system: applications in bacterial localisation studies. Curr Gene Ther;12:12–19.
17. Nijvipakul S., Wongratana J., Suadee C., Entsch B., Ballou D.P., Chaiyen P. (2008) LuxG is a functioning flavin reductase for bacterial luminescence. J Bacteriol;190:1531–1538.
18. Kassem I., Splitter G., Miller S., Rajashekara G. (2014) Let there be light! Bioluminescent imaging to study bacterial pathogenesis in live animals and plants. In: Thouand G., Marks R., editors. Bioluminescence: Fundamentals and Applications in Biotechnology - Volume 3, Volume 154 of the series. Adv Biochem Eng Biotechnol. Berlin: Springer; p.119–145.
19. Close D.M., Patterson S.S., Ripp S., Baek S.J., Sanseverino J., Sayler G.S. (2010) Autonomous bioluminescent expression of the bacterial luciferase gene cassette (lux) in a mammalian cell line. PLoS One;5:e12441.
20. Qian J., Xu Y., Qian X., Zhang S. (2009) A pair of regio-isomeric compounds acting as molecular logic gates with different functions. J Photochem Photobiol, A;207:181–189.
21. Liu T.K., Hsieh P.Y., Zhuang Y.D., Hsia C.Y., Huang C.L., Lai H.P., Lin H.S. *et al.* (2014) A rapid SNAP-tag fluorogenic probe based on an environment-sensitive fluorophore for no-wash live cell imaging. ACS Chem Biol;9:2359–2365.
22. Chen Y., Zhu C., Cen J., Li J., He W., Jiao Y., Guo Z. (2013) A reversible ratiometric sensor for intracellular Cu^{2+} imaging: metal coordination-altered FRET in a dual fluorophore hybrid. Chem Commun;49:7632–7634.
23. Wang W., Li X., Wang J., Xiang S., Feng X., Yang K. (2013) An engineered strong promoter for streptomycetes. Appl Environ Microbiol;79:4484–4492.
24. Gibson D.G., Young L., Chuang R.Y., Venter J.C., Hutchison C.A. 3rd, Smith H.O. (2009) Enzymatic assembly of DNA molecules up to several hundred kilobases. Nat Methods;6:343–345.
25. Ando Y., Niwa K., Yamada N., Irie T., Enomoto T., Kubota H., Ohmiya Y. *et al.* (2007) Development of a quantitative bio/chemiluminescence spectrometer determining quantum yields: re-examination of the aqueous luminol chemiluminescence standard. Photochem Photobiol;83:1205–1210.
26. Niwa K., Ichino Y., Kumata S., Nakajima Y., Hiraishi Y., Kato D., Viviani V.R. *et al.* (2010) Quantum yields and kinetics of the firefly bioluminescence reaction of beetle luciferases. Photochem Photobiol;86:1046–1049.

Supporting Information

Additional Supporting Information may be found in the online version of this article:

Appendix S1. NMR spectra, HR-MS, HPLC, fluorescence spectra, and summary of luminescence and optical

properties. These materials are provided as supporting information and can be found in the online version of this article.

Figure S1. Fluorescence spectra of the compounds.

Figure S2. The composition of the plasmid pCS26-luxAB.

Table S1. Luminescence and optical properties of all compounds.